Received: 16 May 2023 | *Revised:* 21 July 2023 | *Accepted:* 24 July 2023
DOI: 10.37917/ijeee.20.1.5 *Vol. 20 | Issue 1 | June 2024*

Iraqi Journal for Electrical and Electronic Engineering
Original Article

Open Access
IJEEE University of Basrah College of Engineering

Design and Implementation of a 3RRR Parallel Planar Robot

Ammar Aldair *[1], Auday Al-Mayyahi [1], Zainab A. Khalaf [2] and Chris Chatwin [3]
[1]Department of Electrical Engineering, College of Engineering, University of Basrah, Iraq;
[2]Department of Computer Science, College of Education of Pure Science, University of Basrah, Iraq;
[3]Department of Engineering and Design, School of Engineering and Informatics, University of Sussex, UK;

Correspondance
*Ammar Aldair
Department of Electrical Engineering
College of Engineering, University of Basrah, Iraq
Email: ammar.abdulhameed@uobasrah.edu.iq

Abstract
Parallel manipulators have a rigid structure and can pick up the heavy objects. Therefore, a parallel manipulator has been developed based on the cooperative of three arms of a robotic system to make the whole system suitable for solving many problems such as materials handling and industrial automation. The three revolute joints are used to achieve the mechanism operation of the parallel planar robot. Those revolute joints are geometrically designed using an open-loop spatial robotic platform. In this paper, the geometric structure with three revolute joints is used to drive and analyze the inverse kinematic model for the 3RRR parallel planar robot. In the proposed design, three main variables are considered: the length of links of the 3RRR parallel planar robot, base positions of the platform, and joint angles' geometry. Cayley-Menger determinants and bilateration are proposed to calculate these three variables to determine the final position of the platform and to move specific objects according to given desired trajectories. The proposed structure of the 3RRR parallel planar robot is simulated and different desired trajectories are tested to study the performance of the proposed stricter. Furthermore, the hardware implementation of the proposed structure is accomplished to validate the design in practical terms.

Keywords
Parallel Manipulators, Cayley-Menger determinants, Kinematic Characteristics, Bilateration.

I. Introduction

Parallel manipulators (PM) are a closed-loop mechanism consists of two platforms: one is a mobile point, namely, mobile end-effector and the other base platform, called a fixed base. These platforms are linked together by at least two independent arms or chains. The importance of closed-loop mechanism over the open-loop one falls in achieving precision performance, better structural rigidity, reduced inertia of moving parts, and high load-bearing capacity. Due to those advantages, researchers and industrial sectors have been applying parallel manipulators in many important applications. Based on the types of utilized joints which are used to create the kinematic chains that connects the mobile and fix platform , the PM is classified into seven types of configuration [1]: PPR, PRR, RRR, RRP, RPP, RPR, and PRP where P refers to Prismatic joint and R refers to Revolute joint. Typically, the three degrees of freedom planar 3-Revolute–Revolute–Revolute (3RRR) parallel robot is generally composed of mobile end-effector (MEE) and three fixed points that are connected by three manipulator arms, each arm consisting of two free links that are connected by revolution joint. At each fixed point, a motor is used to actuate the arm. The axes of the three revolution joints intersect at a common point called the center of rotation. Actuators are used to change the angles of the parallel manipulator arms provides three degrees of freedom rotational motion that produce changing the location of MEE.

Because of all of its features, the 3RRR parallel planar robot has several advantgaes such as simple structure, accurate positioning, and good symmetry. The 3RRR parallel planar robots are suitable for fast and accurate operations such as material handling; orienting devices, machining application, and medical instrument alignment [2], [3].

Over the last two decades, robotic manipulators have received an observable attention from scientists and industries to increase the automation of workspace and improve of the automation of industrial applications. Robotic manipulators can be constructed into three major structures: parallel, parallel and hybrid manipulators. The first configuration is the serial manipulator [4] and it is an open-loop manipulator because an end is connected to fixpoint while the other end can freely move to any desired location in workspaces. This configuration has the capability to perform a high degree of freedom as a result of the number of links. Such a configuration is widely applied in industrial applications. The second configuration is a closed loop mechanism, namely, a parallel mechanism [5]. Parallel manipulators configurations have superiority over serial manipulators in many applications because they have excellent dynamic responses and high accurate operations. As result, the parallel manipulators have little movement inertia, good structural stiffness, and no cumulative error. Therefore, they are mainly used in special applications which they would require high speed, accuracy, and stiffness [6]. The third configuration is implemented based on both of parallel and serial configurations. Additionally, it could be a combination of multiple parallel configurations [7]. Examples of the third types are Universal-Revolute-Universal (3URU) and Spherical-Revolute-Universal (3SRU) [8].

To study the movement of parallel manipulators, two types of a mathematical model should be derived, the first model is called a forward kinematic model and the other is called an inverse kinematic model. The forward kinematic model is used to find the position of the end-effector of the parallel manipulators depending on the changing of the kinematic parameters such as angles of joints and the length of links. On the other hand, the inverse kinematic model is used to calculate the kinematic parameters that should be set to move the end-effector to the desired position in the workspace. Significant efforts are devoted to derive and analyze forward and inverse kinematic models of 3RRR parallel planar robots that are reported in [9],[10],[11],[12],[13] and [14]. While many other researchers proposed and developed different approaches to design a precise control system for 3RRR planar parallel robotic platform. In reference [15], a predictive control system model is proposed to move the end-effector of a 3-RRR planar parallel robotic platform on the desired path. In reference [16], a hybrid controller comprises two components that were modified to control the position of a 3RRR trajectory. In reference [17], Fuzzy Sliding Mode Controller and optimizing parameters by a genetic algorithm which is introduced to achieve the best-optimized quality control for the 3RRR planar robotic. In reference [18], [19], the accuracy of a 3RRR planar robotic was improved using a developed control technique based on extra array sensors in the implemented passive joints. In reference [20],[21] and [22], direct kinematic solutions to three degrees of freedom planar robotic were introduced.

There is still room to improve and design a control system of a developed 3RRR parallel planar robot. Based on the simplicity of mechanical structure, a designed control system could be capable of solving locomotion problems and provide a high accuracy. In this work, a new algorithm based on both bilateration abd Cayley-Menger determinants is developed to design a control system for locomotion of a 3RRR parallel planar robot to solve locomotion problems and increase the ability of its end-effector to fellow the complex desired path trajectory. To perform this mission, first of all, inverse kinematics of the 3RRR planar parallel robot has been derived to test its performance based on the proposed algorithm. Finally, the implemented structure of the 3RRR planar parallel robotic platform has been integrated with embedded circuits to perform given real-time scenarios.

The conducted works in this paper are firstly introducing a new topology which allows two-way direction movements to reach a particular position and this enhance flexibility in automation of industry. Secondly, we have utilized a new microcontroller what is so called “Polou Maestro Control Centre”. This introduces an individual control for each servo to reach the required position based on the platform movement. Thirdly, we have achieved interfacing between the microcontroller and a computer in which commands have been sent from the computer to the utilized microcontroller. Thus, this increases the flexibility of industrial robots based on the designed robotic system for manufacturing tasks such as pick-and-place, sorting and accurate positioning.

The rest of the paper is structured as follows: Section II presents Cayley-Menger determinants and bilateration while Section III analyses both forward and inverse kinematic models of the 3RRR. The simulation of the 3RRR platform has been investigated in Section IV. The practical experiments have been conducted in Section V. Finally, the conclusion is summed up in Section VI.

II. Cayley-Menger Determinants and Bilateration

A Euclidean metric equation is introduced in a form of polynomial representation; the polynomials can be presented as in the given matrix below which introduces a determinant

of sequences of points e.g. $P_{a1},\ldots P_{an}$ and $Q_{b1},\ldots\ldots Q_{bn}$. The geometric interpretation of those points represents an important element in distance geometry. This determinant is known as Cayley-Menger determinants [23],[24] and [25]. The main advantages of this modeling in relation to the classic formalisms are to introduce bi-direction movements and more precise positioning.

$$D(P_{a1},...,P_{an};Q_{b1},...,Q_{bn}) = 2(\frac{-1}{2})^n \begin{vmatrix} 0 & 1 & . & . & 1 \\ 1 & S_{P_{a1},Q_{b1}} & . & . & S_{P_{a1},Q_{bn}} \\ . & . & & & \\ . & . & & & \\ . & . & & & \\ 1 & S_{P_{an},Q_{b1}} & . & . & S_{P_{an},Q_{bn}} \end{vmatrix} \quad (1)$$

where s_{P_a1,Q_b1}=$\|P_{a1}-Q_{b1}\|^2$ which is independent from the chosen reference frame. In most cases, the two sequences of points are similar, it will be convenient to abbreviate

$D(P_{a1},\ldots,P_{an};Q_{b1},\ldots,Q_{bn})$ by $D(P_1,\ldots,P_n)$ which is so called Cayley–Menger determinant. The $D(P_1,\ldots,P_n)$ is $((n-1)!)^2$ times the squared hypervolume of the spanned by the point $P_1,\ldots,P_n$ in $\Re^{(n-1)}$. Hence, for two points $P_a,P_b(i.e.n=2),D(P_a,P_b)=d(P_a,P_b)^2$, where $d(P_a,P_b)$ is the Euclidean distance between P_a and P_b. For three points $P_aP_bP_c(i.e.n=3),D(P_aP_bP_c)=\mp\frac{1}{2}\sqrt{(D(P_aP_bP_c))}$ is the sign area of the triangle $P_aP_bP_c$ (shown in Fig. 1(a)),where the $\mp$ sign accounts for the two mirror locations of P_c respect to the line defined by P_aP_b. The two vectors $P_aP_b and P_aP_c$ can be expressed by scalar product as: $D(P_aP_b;P_aP_c)=(P_a-P_b).(P_a-P_c)$.This dot product is computed as $d(P_a,P_b)d(P_a,P_b)\cos\theta$,with θ being the angle between the lines P_aP_b and P_aP_c. The angle (θ) between P_aP_b and P_aP_c can be calculated from the following formula:

$$\theta=\cos^{-1}\left(\frac{D(P_aP_b;P_aP_c)}{D(P_a,P_b)D(P_a,P_b)}\right) \quad (2)$$

where $D(P_aP_b;P_aP_c)$ represents the scalar product between the two vectors P_aP_b and P_aP_c.

The bilateration representation [26], [27] is a geometric problem which is introduced using Cayley-Menger determinants. To allocate the locations of a point Pc (shown in Fig. 1(b)), its distances can be assumed to two other points, Pa and Pb, whose locations are known. The projected vectors of those points are demonstrated in Figure 1(b).

Hence, orthogonal vector Pc could be projected onto P_aP_b so that the obtained position vector can be expressed as follows:

$$\begin{aligned} P &= P_a+\sqrt{\frac{D(P_a-P_c)}{D(P_a-P_b)}}\cos\theta(P_b-P_a) \\ &= P_a+\frac{D(P_aP_b;P_aP_c)}{D(P_a-P_b)}(P_b-P_a) \end{aligned} \quad (3)$$

Moreover, the position vector of the Pc can be formulated as follows

$$P_c=P\mp\sqrt{\frac{D(P_aP_bP_c)}{D(P_a-P_b)}}S(P_b-P_a) \quad (4)$$

where $S=\begin{bmatrix}0 & -1\\ 1 & 0\end{bmatrix}$ and the $\mp$ sign represents two mirror-symmetric locations of P_c in respect of the defined line by the vector $\overline{P_aP_b}$. By substituting Equation no. (3) into Equation no. (4), the following equation can be obtained

$$\begin{aligned} P_c &= P_a+\frac{D(P_aP_b;P_aP_c)}{D(P_a-P_b)}I_2(P_b-P_a) \\ &\quad \mp\sqrt{\frac{D(P_aP_bP_c)}{(D(P_a-P_b))^2}}S(P_b-P_a) \end{aligned} \quad (5)$$

where: I_2 is 2 by 2 identity matrix. Thus,

$$\begin{aligned} (P_c-P_a) = \frac{1}{D(P_a-P_b)}&(D(P_aP_b;P_aP_c)I_2 \\ &\mp\sqrt{D(P_aP_bP_c)}S)(P_b-P_a) \end{aligned} \quad (6)$$

Equation no. (6) denotes to a bilateration problem as a function of Cayley-Menger determinants. Additionally, another possible representation can be expressed based on this matrix as follows:

$$(P_c-P_a)=Z_{a,b,c}(P_b-P_a) \quad (7)$$

where

$$\begin{aligned} Z_{a,b,c} &= \frac{1}{D(P_a-P_b)}(D(P_aP_b;P_aP_c)I_2\mp\sqrt{D(P_aP_bP_c)S)} \\ &= \frac{1}{D(P_a-P_b)}\begin{pmatrix} D(P_aP_b;P_aP_c) & \mp\sqrt{D(P_aP_bP_c)} \\ \mp\sqrt{D(P_aP_bP_c)} & D(P_aP_b;P_aP_c)\end{pmatrix} \end{aligned} \quad (8)$$

$Z_{a,b,c}$ is defined as the bilateration matrix.

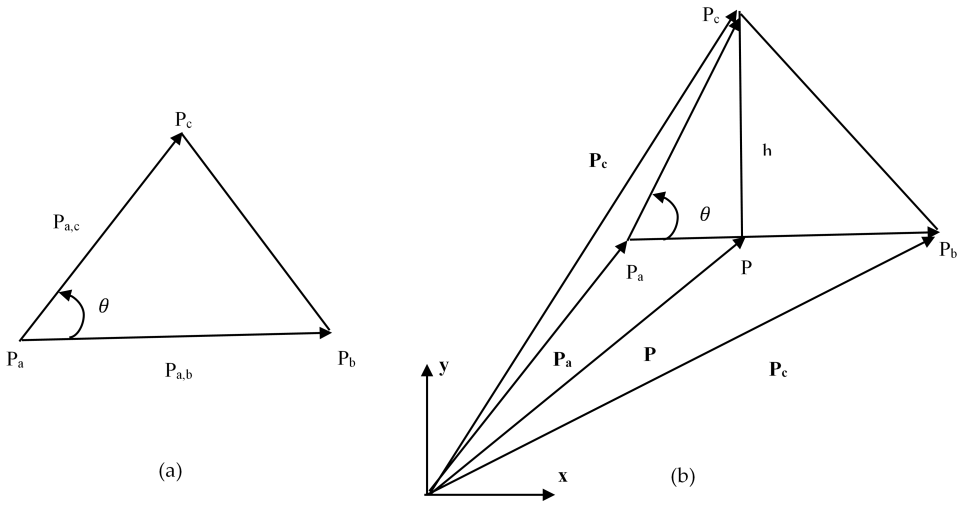

Fig. 1. Bilateration representation (a) geometric problem (b) vectors projection.

III. Kinematics Model for 3RRR Parallel Robot

The platform structure of the 3RRR planar parallel robotic is shown in Fig. 2. The topology of the 3RRR is generally composed of single MEE and three fixed based points each point is called actuated (or active) point because it is attached to a servo motor. The active point (point A_i $i \in (1\ 2\ 3)$) is connected by three identical manipulator arms, each arm consisting of two free links (l_{1i} and l_{2i}) that are connected by revolution joint at the point B_i it is called a passive point.The axes of the three revolution joints intersect at a common point called the center of rotation (point E). The servo motors are used to change the angles of the parallel manipulator arms provides three degrees of freedom rotational motion that produce changing the location and orientation of MEE. The kinematics model for 3RRR parallel planar robot is classified into two models: the forward kinematic model and the inverse kinematic model. In this section, the forward and inverse kinematic are derived.

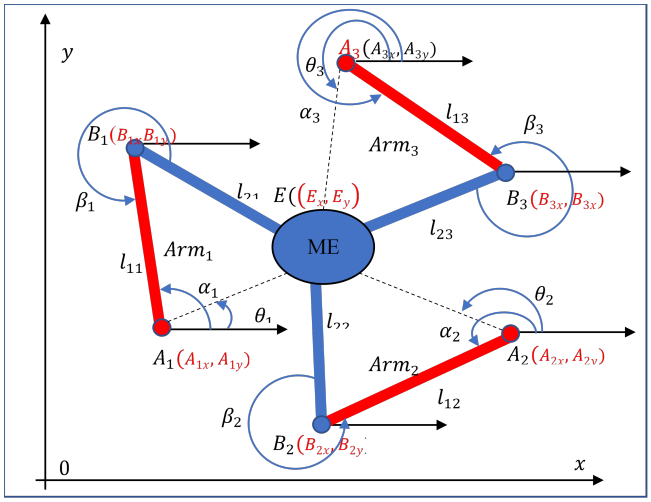

Fig. 2. The structure of 3RRR planar parallel robotic platform.

A. *The Forward Kinematic Model of 3RRR Parallel Planar Robot*

This model is used to find the coordinate of the MEE (E_x, E_y, σ) depending on values of kinematic parameters (length of active links l_{1i}, length of passive links l_{2i}, angles active links α_i, the coordinate of active points (A_{ix}, A_{iy}) and the coordinate of passive points (B_{ix}, B_{iy}). From Fig. 3, the following independent equations can be derived to describe the workspace of the MEE of the 3RRR parallel planar robot as shown below:

$$l_{21}^2 = \sqrt{(E_x - B_{1x})^2 - (E_y - B_{1y})^2} = D(B_1, E) \quad (9)$$

$$l_{22}^2 = \sqrt{(E_x - B_{2x})^2 - (E_y - B_{2y})^2} = D(B_2, E) \quad (10)$$

$$l_{23}^2 = \sqrt{(E_x - B_{3x})^2 - (E_y - B_{3y})^2} = D(B_3, E) \quad (11)$$

The above set of equation can be rewritten as below:

$$\Re_1 E_x + \Re_2 E_y + \Re_3 = D(B_2, E) - D(B_1, E) \quad (12)$$

$$\Re_4 E_x + \Re_5 E_y + \Re_6 = D(B_3, E) - D(B_1, E) \quad (13)$$

where:
$\Re_1 = 2B_{1x} - 2B_{2x}$
$\Re_2 = 2B_{1y} - 2B_{2y}$
$\Re_3 = (B_{2x}^2 + B_{2y}^2) - (B_{1x}^2 + B_{1y}^2)$
$\Re_4 = 2B_{1x} - 2B_{3x}$
$\Re_5 = 2B_{1y} - 2B_{3y}$
$\Re_6 = (B_{3x}^2 + B_{3y}^2) - (B_{1x}^2 + B_{1y}^2)$

By rearranging the above equations, the coordinate of the MEE (E_x ,E_y) can be computed as:

$$\begin{bmatrix} E_x \\ E_y \end{bmatrix} = \begin{bmatrix} \Re_1 & \Re_2 \\ \Re_4 & \Re_5 \end{bmatrix}^{-1} \begin{bmatrix} D(B_2,E) - D(B_1,E) - \Re_3 \\ D(B_3,E) - D(B_1,E) - \Re_6 \end{bmatrix} \quad (14)$$

The Eqn. (14) for the forward kinematic provides a unique solution, i.e., the joint angle variables are known, the position of the MEE will be determined. The orientation of the MEE can be calculated using the equation below:

$$\begin{bmatrix} B_{ix} \\ B_{iy} \end{bmatrix} = \begin{bmatrix} (A_{ix} + \sqrt{D(B_i,A_i)}\cos(\alpha_i) \\ (A_{iy} + \sqrt{D(B_i,A_i)}\sin(\alpha_i) \end{bmatrix} \quad (15)$$

B. *The Inverse Kinematic Model of 3RRR Parallel Planar Robot*

The inverse kinematic model is used to calculate the angles α_i that should be set to compute the coordinate of mobile end-effector and move MEE along a desired trajectory in the workspace. From Fig. 2, in the triangle $A_iB_iE_i$, the relationship between the angles α_i and the point E can be computed from the following equation:

$$\sigma = \tan^{-1}(\frac{E_y}{E_x}) \quad (16)$$

The angle θ_i and length A_iE can be computed from the following equations:

$$D(B_i,E) = D(B_i,A_i) + (A_iE)^2 - 2\sqrt{D(B_i,A_i)}(A_iE)\cos(\alpha_i - \theta_i) \quad (17)$$

$$\theta_i = \tan^{-1}\left(\frac{E_y - A_{iy}}{E_x - A_{ix}}\right) \quad (18)$$

$$A_iE = \sqrt{(E_y - A_{iy})^2 + (E_x - A_{ix})^2} = D(A_i,E) \quad (19)$$

From Eqns. (16), (17) and (18) the angles α_i can be found as:

$$\alpha_i = \tan^{-1}\left(\frac{D(B_i,A_i) + (A_iE)^2 - D(B_i,E)}{2\sqrt{D(B_i,A_i)}(A_iE)}\right) \quad (20)$$

Based on the kinematics model for 3RRR Parallel Planar Robot i.e. forward and inverse kinematic models, is to design a precise controller for parallel manipulator robot. The required control signals can be identified and applied for each servo motors to force the mobile end-effector to move along a desired trajectory in a given workspace. Moreover, some variables of mobile end-effector such as the linear speed and angular speed can be computed easily from Eq. (19) which represent the position. Additionally, for the inverse kinematics, there are different angle settings of the joints that lead to the same position of the MEE based on Eq. (20).

Depending on the mathematical equation of the desired trajectory e.g. mathematical equation of circular trajectory is $x = r\cos\theta, y = r\sin\theta$, the inverse kinematic model of 3RRR parallel planar robot will generate the desired angles ($\alpha_i where i \in (1\ 2\ 3)$) from Eq. (20). Additionally, based on the generated desired angles, the controller will provide control signals which are applied to actuators fixed in the active points (A_i). Hence, the actuators will generate the actual angles and those generated actual angles will be used as the input to the forward kinematic model of 3RRR parallel planar robot, this model is responsible to derive the MEE to draw the actual trajectory depending on Eq. (14).

IV. Simulation Results

To investigate the performance of the proposed model of the 3RRR parallel planar robot, the geometric structure of the derived kinematic model of the given robot is simulated using the MATLAB codes. Figure 3 shows the simulated topology of the 3RRR parallel planar Robot.

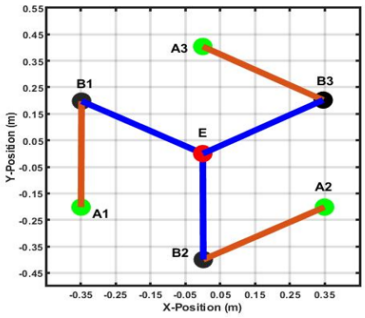

Fig. 3. The topology of 3RRR planar parallel robot using MATLAB environment.

From Fig. 3, the locations of servo motors (active points) are: A_1 (-0.35,-0.2), A_2 (0.35,-0.2) and A_3 (0,0.4), respectively and the measurement units of these positions are in meters. The length of the active link is l_{1i}=0.4 (m) and the length of the passive link is l_{2i}=0.4 (m). These links are chosen based on the prototype of the workspace. The parallel manipulator

is a closed-loop mechanism consists of three serial chains that connecting the active revolute joints A_i to the mobile end-effector E (revolute joint) via passive revolute joints B_i. The workspace of the 3RRR parallel planar Robot is the area where the mobile end-effector can move through. Figure 5 shows the workspace environment of the 3RRR parallel manipulator which it limits the movement of the end effector. The obtained workspace has three curved pieces each curve is constructed from intersecting of two circles one has a radius $(l_{1i}+l_{2i})$ and centered at A_i and the other circle has a radius $(l_{1i}-l_{2i})$ and centered at A_i. By applied the trajectory shown in Figure 4 as reference to the inverse kinematic model, the angle arms of each base joint of the 3RRR platform obtained from Eq. (20) above will generated by the three servo motors to construct this trajectory accordingly as shown in Fig. 5.

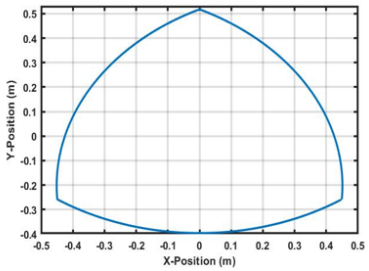

Fig. 4. The workspace of 3RRR planar parallel robot

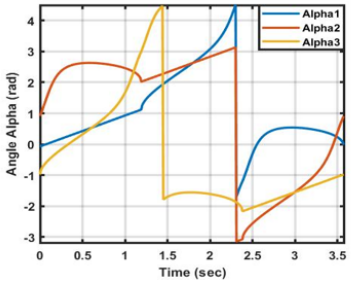

Fig. 5. Angle arms of each base joint of 3RRR planar parallel robot.

Trajectories can be divided as a continuous one such circular or sinusoidal and as discontinuous trajectories such square and triangular. The main difference is the sharp angles that exist in the non-continuous trajectories which may cause a jump in the turning at sharp angles. Therefore, two trajectories have been tested to evaluate the performance of the 3RRR planar parallel robot. The first trajectory is a circular path as shown in Fig. 6 and it has radius 0.3m and centered at the origin coordinates. Fig. 7 shows the angle arms of each base joint of the 3RRR platform that is generated by the servo motors to move the end-effector along this circular path. The second trajectory is the triangular one and it is equilateral and side length equals to 0.55m, which has sharp convex points as shown in Fig. 8 Similarly, Fig. 9 shows the angle arms of each base joint of the 3RRR platform that are generated to move the end-effector along the triangular path. It is observable that that the 3RRR planar parallel robot can follow variety of trajectories as demonstrated in the aforementioned figures. This has successfully proven the effectiveness of the proposed system in satisfying the performance smoothly and feasibly. The performance criterion can be understood by tracking the given reference trajectories as required.

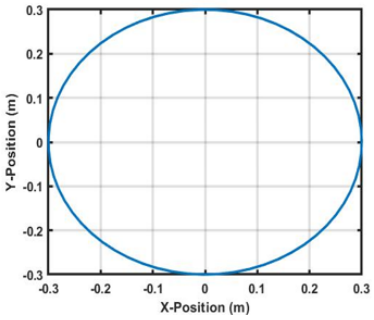

Fig. 6. The circular path followed by 3RRR planar parallel robot

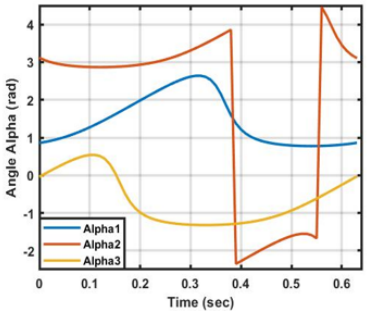

Fig. 7. The generated angles by servo motors to make the MEE follows the circular path

V. Real-Time Implementation and Experiments

The hardware implantation is done by assembling the main components represented by servo motors, arms and a microcontroller. The used microntoller is called a Polou Maestro Control Center as demonstrated in Fig. 10 below which is utilized to control the rotation limits of servo motors and their speeds. Each servo can have as specific number as an input as depicted in Fig.11. The serial communication used in the Polou Maestro Control Center is based on ”UART type as

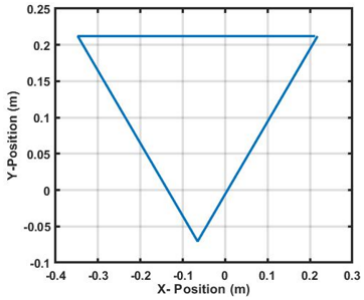

Fig. 8. The triangle path followed by 3RRR planar parallel robot

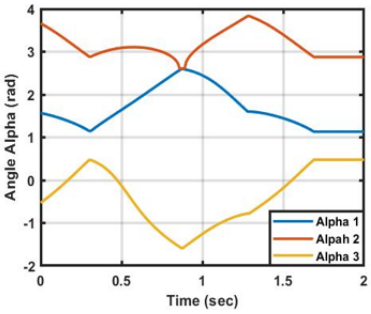

Fig. 9. The generated angles by servo motors to make the MEE follows the triangular

shown in the setting tab provided in in Fig. 12. The baud rate is set to 9600 to speed up the communication. The computer specifications used in our experiments are CPU is 1.6GHz, core i5 and RAM equals 4GB.

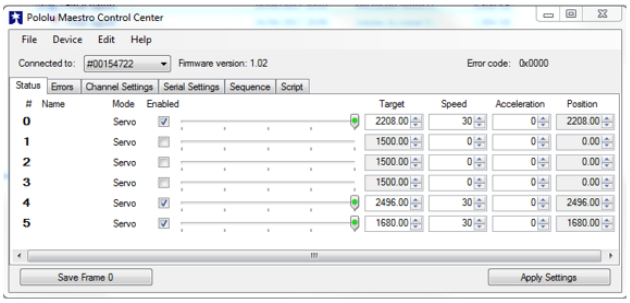

Fig. 10. Controlling servos using Pololu Masestro

After conducting of all aforementioned requirements, we have assembled all electrical and mechanical components of the 3RRR planar robot. Figure 13 demonstrates the assembly of the manufactured components with each other to make the desired structure. To investigate the effectiveness of the overall performance, three case studies conducted based on practical experiments as in the following subsection:

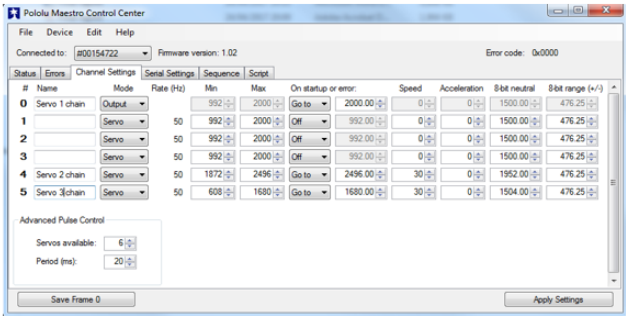

Fig. 11. The channel setting of servos

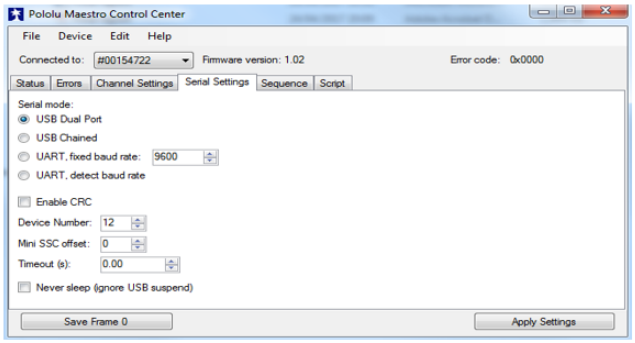

Fig. 12. The serial communication between the PC and the Maestro controller.

A. *Case study -1: Triangular Trajectory*

In this case study, a triangular movement will be tested to validate the effectiveness of the platform movement as demonstrated in Fig.14. The movements of the platform based on the time responses of both X and Y axes are shown in Figs. 15 (a) and (b), respectively. When the MEE moves, the coordinates of X and Y change accordingly within the area of workspace and this proves the design and satisfies the operating condition practically.

B. *Case study-2: Circular Trajectory*

To examine the adaptation of the system in case of different trajectory, a circular path is studied. It can be clearly noticed that the MEE is capable of tracking the given path feasibly and validate the time response as shown in Fig. 16. Additionally, the time responses of the X and Y axes for the circular trajectory are depicted in both Figs. 17 (a) and (b), respectively. The input commands are received from the PC and supplied to the microcontroller. This, as a result, will general the required signature which provided to the actuation servo motors. Thus, the movement will occur accordingly.

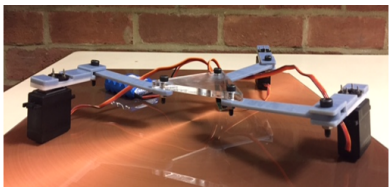

Fig. 13. The practical implementation of the 3RRR parallel planar robot

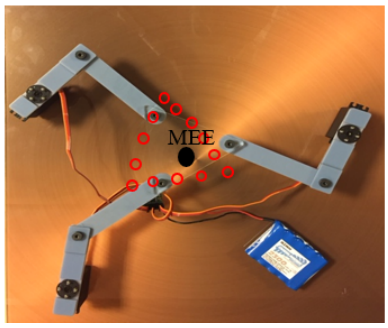

Fig. 14. The movement of the 3RRR parallel planar robot in case of triangular trajectory.

C. Case study-3: Complex Trajectory

Furthermore, a complex trajectory has been applied which combines both continuous and none continuous paths. In other words, sharp turning and smooth tracking are found to demonstrate and validate the movement the system. This case study is described as shown in Fig. 18. Moreover, the time response of X and Y coordinates are shown in Fig. 19. These graphs are changed continuously as observed in which the complex trajectory is obtained. In real life, such a trajectory can be used in computer numerically controlled machine.

VI. Conclusions

In this research, the 3RRR parallel planar robot has been analyzed using the inverse kinematic model by which the 3RRR can perform specific positions. Those positions are implemented based on three trajectories i.e., triangular, circular and complex one. For each trajectory, the performance of the system has shown a successful tracking to the target points. Both simulation and experiments results have been obtained to verify the functionality in terms of practical aspect based on the given paths. The inverse kinematics model in additional to Cayley-Menger determinants and bilateration analytic have make the system able to reach the destination trajectory. In the future work, we will be designing a control strategy to improve the overall performance further.

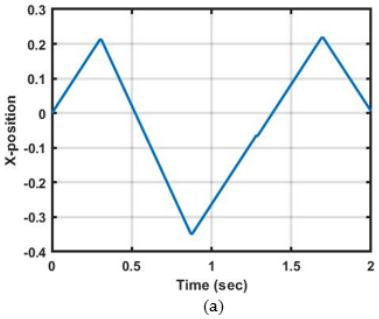

(a) for X-axis

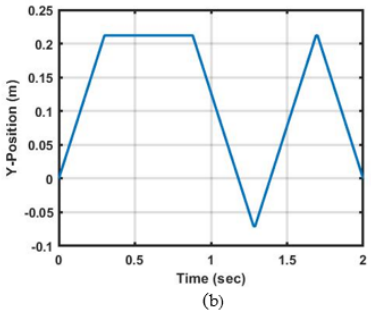

(b) for Y-axis

Fig. 15. The coordinates response of the triangular trajectory

Conflict of Interest

The authors have no conflict of relevant interest to this article.

References

[1] A. K. Dash, I.-M. Chen, S. H. Yeo, and G. Yang,, "Task-oriented configuration design for reconfigurable parallel manipulator systems," *Int. J. Comput. Integr. Manuf*, vol. 18, no. 7, pp. 615–634, 2005.

[2] F. G. Salas, V. Santibanez, and M. A. Llama, "Fuzzy-tuned pd tracking control of a 3-rrr parallel manipulator: Stability analysis and simulations," *Intell. Autom. Soft Comput*, vol. 20, no. 2, pp. 159–182, 2014.

[3] R. Wang and X. Zhang, "Parameters optimization and experiment of a planar parallel 3-dof nanopositioning system," *IEEE Trans. Ind. Electron*, vol. 65, no. 3, pp. 2388–2397, 2018.

[4] Z. Li, M. Brandstotter, and M. Hofbaur, "Kinematic analysis for a planar redundant serial manipulator in multibody mechatronic systems," *Springer International Publishing*, pp. 97–106, 2018.

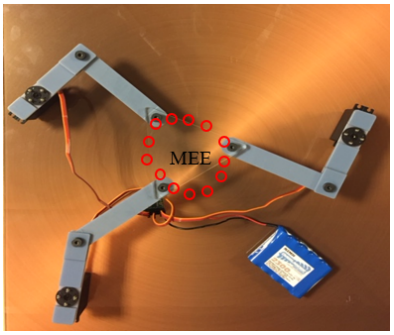

Fig. 16. The movement of the 3RRR parallel planar robot in case of circular trajectory.

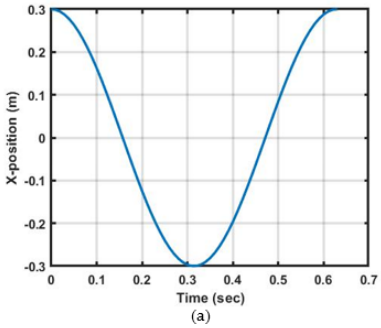

(a) for X-axis

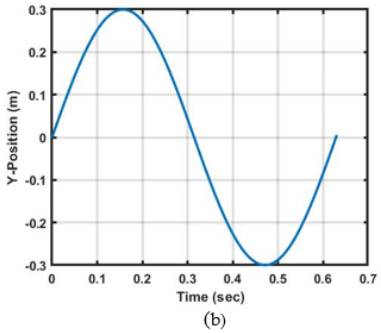

(b) for Y-axis

Fig. 17. The coordinates response of the circular trajectory

[5] A. A. Aldair and W. Wang, "Neural controller based full vehicle nonlinear active suspension systems with hydraulic actuators," *International Journal of Control and Automation*, vol. 4, no. 2, pp. 79–94, 2011.

[6] O. Hamdoun, L. El Bakkali, and F. Z. Baghli, "Analysis and optimum kinematic design of a parallel robot," *Procedia Eng*, vol. 181, pp. 214–220, 2017.

[7] G. Coppola, D. Zhang, and K. Liu, "A 6-dof reconfigurable hybrid parallel manipulator," *Robot. Comput. Integr. Manuf*, vol. 30, no. 2, pp. 99–106, 2014.

[8] B. N. AbdulSamed , A. A. Aldair, , A. Al-Mayyahi, "Robust trajectory tracking control and obstacles avoidance algorithm for quadrotor unmanned aerial vehicle," *Journal of Electrical Engineering and Technology*, vol. 15, no. 2, pp. 855–868, 2020.

[9] I. Bonev, S. Briot, P. Wenger, and D. Chablat, "Changing assembly modes without passing parallel singularities in non-cuspidal 3-rpr planar parallel robots," *in The Second International Workshop on Fundamental Issues and Future Research Directions for Parallel Mechanisms and Manipulators*, pp. 1–4, 2008.

[10] S. Staicu, Kinematics of the 3-RRR planar parallel robot, UPB Sci. Bull. Ser. D Mech. Eng., vol. 70, no. 2, pp. 3-14, 2008.

[11] I. A. Bonev, D. Zlatanov, and C. M. Gosselin,, "Singularity analysis of 3-dof planar parallel mechanisms via screw theory," *J. Mech. Des.*, vol. 125, no. 3, p. 573, 2003.

[12] M. Rodelo, J. L. Villa, J. Duque, and E. Yime, "Kinematic analysis and performance of a planar 3rrr parallel robot with kinematic redundancy using screw theory," *in The IEEE 2nd Colombian Conference on Robotics and Automation*, 2018.

[13] S. Kucuk, "Energy minimization for 3-rrr fully planar parallel manipulator using particle swarm optimization," *Mech. Mach. Theory*, vol. 62, pp. 129–149, 2013.

[14] A. Al-Mayyahi, A. A. Aldair, and C. Chatwin, "Control of a 3-rrr planar parallel robot using fractional order pid controller," *Int. J. Autom. Comput*, vol. 17, pp. 822–836, 2020.

[15] A. K. Dash, S. Krishnamurthy, S. Prasadh, and V. Sundar, "Position control of a 3-rrr planar parallel manipulator with non-planar links using external encoders," *Adv. Mater. Res*, vol. 971-973, pp. 1280–1283, 2014.

[16] S. X. Tian and S. Z. Wang, "Hybrid position/force control for a rrr 3-dof manipulator," *Appl. Mech. Mater.*, vol. 48-49, pp. 589–592, 2011.

[17] V. D. Vuong, N. Q. Hoang, and N. T. Duy, "Control parallel robots driven by dc motors using fuzzy sliding mode controller and optimizing parameters by genetic algorithm," *in International Conference on Engineering Research and Applications*, pp. 202–214, 2019.

[18] A. Zubizarreta, M. Marcos, I. Cabanes, C. Pinto, and E. Portillo, "Redundant sensor based control of the 3rrr

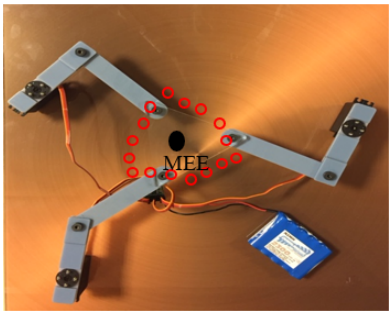

Fig. 18. The movement of the 3RRR parallel planar robot in case of complex trajectory.

parallel robot," *Mech. Mach. Theory*, vol. 54, pp. 1–17, 2012.

[19] C. Fuqing, Z. Sijun, and G. Xijuan, "Kinematical performance analysis for planar parallel mechanism 3rrr," *CHINESE J. Mech. Eng*, vol. 17, pp. 181–184, 2004.

[20] J. R. Gao, Y. Z. Wang, and Z. P. Chen, "Modelling and simulation of inverse kinematics for planar 3-rrr parallel robot based on simmechanics," *Adv. Mater. Res*, vol. 898, pp. 510–513, 2014.

[21] D. Oetomo, H. C. Liaw, G. Alici, and B. Shirinzadeh, "Direct kinematics and analytical solution to 3rrr parallel planar mechanisms," *in The 9th International Conference on Control, Automation, Robotics and Vision*, pp. 1–6, 2006.

[22] F. Thomas and L. Ros, "Revisiting trilateration for robot localization," *IEEE Trans. Robot*, vol. 21, no. 1, pp. 93–101, 2005.

[23] C. D. Andrea and M. Sombra, "The cayley-menger determinant is irreducible for n $\geq$ 3," *Sib. Math. J*, vol. 46, no. 1, pp. 71–76, 2005.

[24] N. Rojas and F. Thomas, "On closed-form solutions to the position analysis of baranov trusses," *Mech. Mach. Theory*, vol. 50, pp. 179–196, 2012.

[25] R. L. Williams and B. H. Shelley, "Inverse kinematics for planar parallel manipulators,," *in ASME Design Technical Conferences*, pp. 1–6, 1997.

[26] N. E. R. Libreros, "Distance-based formulations for the position analysis of kinematic chains," *UNIVERSITAT POLIT ECNICA DE CATALUNYA*, 2012.

[27] N. Rojas and F. Thomas, "The forward kinematics of 3-rpr planar robots: Short papers review and a distance-based formulation," *IEEE Trans. Robot.*, vol. 27, no. 1, pp. 143–150, 2011.

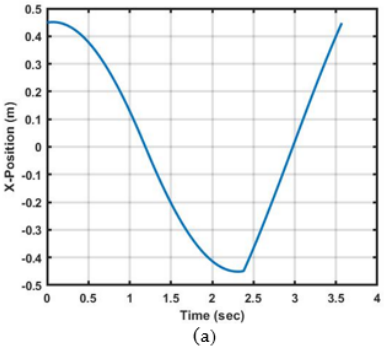

(a) for X-axis

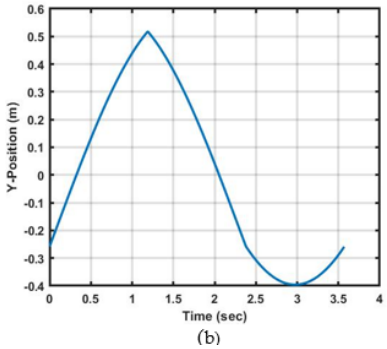

(b) for Y-axis

Fig. 19. The coordinates response of the complex trajectory